photonics

MDPI

Communication

1.1–1.6 μm Multi-Wavelength Random Raman Fiber Laser

Chunhua Hu [1,2] and Ping Sun [1,*]

1 Shandong Provincial Engineering and Technical Center of Light Manipulations & Shandong Provincial Key Laboratory, School of Physics and Electronics, Shandong Normal University, Jinan 250014, China
2 Electrical Engineering College, Binzhou University, Binzhou 256603, China
* Correspondence: sunping@sdnu.edu.cn

Abstract: Multi-wavelength fiber lasers have attracted great attention due to their application value in many fields. In this work, we demonstrated a seven-wavelength random Raman fiber laser in the range of 1.1–1.6 μm. A piece of 1-km-long high Raman gain optical fiber is utilized as the gain medium. The 1st-order to 7th-order Stokes waves are located, respectively, at 1133 nm, 1194 nm, 1260 nm, 1332 nm, 1414 nm, 1504 nm, and 1606 nm. In the 3-dB bandwidth of optical spectra of 1st-order and 2nd-order Stokes waves, four peaks with an average spacing of 1 nm and 20 peaks with an average spacing of 0.45 nm respectively, are recorded. Pumped by a 1080 nm/12.5 W/220 ns laser, the maximum output power can reach 4.16 W, corresponding to the optical-to-optical conversion efficiency of ~30.7%.

Keywords: multi-wavelength fiber laser; Raman fiber laser; random fiber laser; fiber loop mirror

1. Introduction

Multi-wavelength fiber lasers have attracted extensive attention as a result of their great application value in the fields of multi-species gas monitoring, photoacoustic spectroscopy, wavelength-division-multiplexing (WDM) systems, and fiber-optic sensing, etc. [1–3]. The output characteristics of multi-wavelength fiber lasers rely on the lasing procedures and gain mediums used [4]. The gain mediums will affect working stability and wavelength. The procedures reflect the formation mechanisms of multi-wavelength operations. The types of procedures can be divided into passive elements and active nonlinear processes. Fiber Bragg gratings (FBGs) [5,6], fiber loop mirrors [7], Fabry-Perot [8], and Mach-Zehnder [9] interferometer filters are typical and commonly used passive elements. In addition, the nonlinear processes mainly include Stimulated Brillouin scattering (SBS) [10], Stimulated Raman scattering (SRS) [11], random distribution feedback (RDFB) [4], and four-wave mixing (FWM) [12]. The stable operation of multi-wavelength lasers depends on the cooperation of these nonlinear processes and key elements. Multimode, sampled, and phase-shifted FBGs that can reflect multi-wavelengths can all be applied for multi-wavelength operation. Zhang et al. [13] demonstrated a switchable multi-wavelength thulium-doped fiber laser (TDFL) which can obtain ten-wavelength operation with high stability based on a polarization-maintaining sampled FBG. Fabry-Perot interferometer can generate multi-wavelengths when the cavity length and free spectral ranges satisfy the least common multiple number [14]. Wang et al. [15] reported a multi-wavelength TDFL using a Microfiber-optic Fabry-Perot interferometer with a free spectral range of ~26 nm as the wavelength-selective filter. Sierra-Hernandez et al. [16] presented a multi-wavelength erbium-doped fiber laser based on a Mach-Zehnder interferometer, which is constructed by splicing photonic crystal fiber (PCF) between two segments of a single-mode fiber. Based on the interference between modes, fiber loop mirrors can play the role of fiber filters with low loss to generate multi-wavelength lasing oscillations [4]. Liu et al. [17] obtained 15 output channels within 10-dB bandwidth from 1990 nm to 2007.5 nm by utilizing a fiber Sagnac loop mirror based on polarization-maintaining fiber.

check for updates

Citation: Hu, C.; Sun, P. 1.1–1.6 μm Multi-Wavelength Random Raman Fiber Laser. *Photonics* **2023**, *10*, 164. https://doi.org/10.3390/photonics10020164

Received: 21 December 2022
Revised: 26 January 2023
Accepted: 29 January 2023
Published: 3 February 2023

Based on the abovementioned passive elements and active nonlinear processes, various kinds of setups like semiconductor optical amplifiers [18,19], rare-earth-doped fiber lasers [20], and Raman fiber lasers (RFLs) [21,22] have demonstrated that they are excellent tools to obtain multi-wavelength operation. Especially, the advent of random Raman fiber lasers (RRFLs) in 2010 [23] suggests the possibility that fiber can be used as a kind of disorder medium to generate multi-wavelength operation under the action of RDFB and Raman amplification via a long distance. RRFLs have greater attraction as they can realize switching of various customized wavelengths by selecting appropriate Raman gain medium, pump source, and other technical parameters. For example, using a homemade tunable Yb-doped fiber laser (1075 $\pm$ 25 nm) as the pump source, Balaswamy et al. [24] demonstrated a tuning RRFL with a tuning range from 1450 to 1510 nm, based on a reel of 350-m-length high Raman nonlinearity fiber (effective area 12 μm^2) with special filtering properties. Commonly used single-mode fibers are difficult to use for realizing 2 μm RRFLs limited by the low Raman gain at 2 μm and increased propagation loss. So, highly GeO_2-doped silica fibers (higher Raman gain and lower optical loss at 2 μm) with different lengths are used to explore the performance at 2 μm band [25,26]. In addition, Jin et al. [27] reported a 2.1 μm random fiber laser with 150 m highly GeO_2-doped silica fiber. Moreover, RRFLs have good environmental stability, as the weak RDFB from Rayleigh scattering generates via a long piece of passive fiber. However, the previous research mainly focused on the output of Stokes waves of a certain order based on cascaded Raman shifts. Different techniques and structures are used to improve the purity of output spectra by suppressing the starting vibration of other Stokes waves. Only a few reports focus on the multi-wavelength simultaneous output. Kim et al. [22] reported a tunable multi-wavelength all-fiber Raman source working from 1.12–1.58 μm based on a tunable intracavity high birefringence fiber Sagnac loop filter, but the intensity of each Stokes wave varies greatly. Recently, Adamu et al. [1] built a gas-filled fiber Raman laser which can span from 1.53–2.4 μm. However, the use of a part of 5-m-length hydrogen (H_2)-filled nested anti-resonant fiber, all-polarization maintaining master oscillator power amplifier configuration, and the focusing coupling system makes it complicated and high cost.

In this study, we utilize a piece of 1-km-long Raman optical fiber with a high Raman gain efficiency and low Raman threshold as the gain medium to realize a multi-wavelength operation. This Raman optical fiber can provide enough gain at any wavelength from 1100 to 1700 nm. Based on the high Raman gain fiber, a half-open cavity RRFL is built. Combined with a nanosecond pump laser working at 1080 nm, seven wavelengths of 1.1–1.6 μm can output at the same time under the action of SRS. It should be noted that there are four peaks recorded in the 3-dB bandwidth of the optical spectrum (3.57 nm) of the 1st-order Stokes wave, and 20 peaks in the 3-dB bandwidth of the optical spectrum (8.84 nm) of the 2nd-order Stokes wave.

2. Experimental Setup

In order to realize the possibility of multi-wavelength operation in a wide band of optical spectrum, an RRFL with a half-open cavity structure shown in Figure 1 is built. The Raman gain medium used in our work is a piece of 1-km-long Raman optical fiber (from OFS company) with a high index core and a small effective area which are specially designed to yield a high Raman gain efficiency. The core diameter is about 4 μm and the cladding diameter is about 125 μm. The peak Raman gain efficiency is 2.55 $(W\cdot km)^{-1}$. The effective areas of 1450 nm and 1550 nm are 16.2 μm^2 and 18.94 μm^2. Moreover, the threshold of Raman shift of Raman optical fiber is lower compared with standard single-mode fiber of the same length. The pump laser works at 1080 nm. The maximum pump power and pulse width are 12.5 W and 220 ns. A pump combiner is utilized to inject the pump laser into the random Raman cavity. A fiber loop mirror obtained by fusing two output terminals of an output coupler with an output ratio of 50:50 is connected to the signal part of the pump combiner and used as a total reflection mirror. Under the naturally present random distributed feedback (RDFB) along the 1-km-long Raman optical fiber and the broadband-reflective effect of the fiber loop mirror, Raman optical resonators are formed. The output part is cut with an angle of 8 degrees to avoid unexpected backward reflection. The eventual output wavelengths and corresponding output powers depend entirely on the competition of different wavelengths. To ensure the stable operation of the laser, the whole laser is placed on a water-cooled plate, and the set temperature of the water-cooled plate is 20 °C. The output characteristics are recorded by an optical spectrum analyzer (Anritsu, MS9710C, 0.6–1.75 μm), and an optical power meter (Ophir, Starlite-AC Rohs).

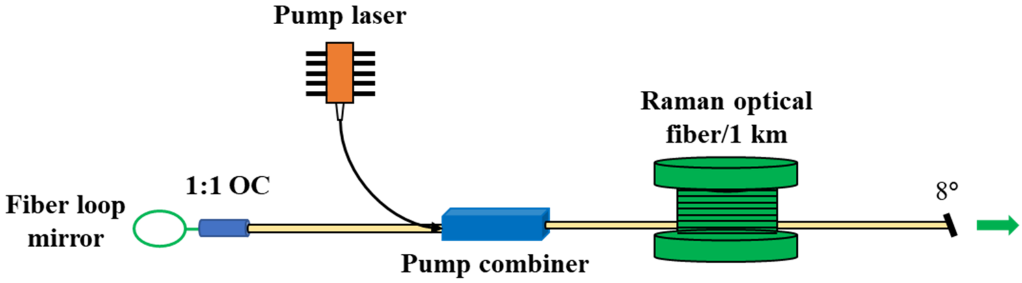

Figure 1. Structure of the multi-wavelength random Raman fiber laser.

3. Experimental Results and Discussion

Based on the setup shown in Figure 1, the multi-wavelength output is realized in our work. Figure 2A exhibits the optical spectrum of the multi-wavelength RRFL. In addition to the fundamental frequency light (pump laser) located at 1080 nm, seven spectral lines from 1st-order to 7th-order Stokes waves corresponding to 1133 nm, 1194 nm, 1260 nm, 1332 nm, 1414 nm, 1504 nm, and 1606 nm can be recorded. The seven Stokes waves can vibrate at the same time since the Raman optical fiber has a low Raman threshold, and the initial pump power (2.6 W) has reached the threshold of any order in the seven Stokes waves. Moreover, the Raman optical fiber can provide relatively uniform Raman gain in the range from 1.1 to 1.7 μm, and the fiber loop mirror does not have the function of selecting specific wavelengths like gratings. So, six Stokes waves can be covered in the intensity range of full width at half maximum (FWHM) of the optical spectrum and have a rather uniform power level. The relation between total output power and pump power is given in Figure 2. The fitting cure has good linearity, and the slope of the fitting curve is ~30.2%. When the pump power is 12.5 W, the output power can reach the maximum value, which is 4.16 W (the residual pump power is about 0.32 W), corresponding to the optical-to-optical conversion efficiency of ~30.7%. Additionally, the output power of different Stokes waves is analyzed, and the experimental results are shown in Figure 3A. As the Raman optical fiber has a large loss for a wavelength over 1.7 μm, higher-order Stokes waves cannot be obtained at the current pump power. The power cannot transfer to higher Stokes waves but only transfer between the seven Stokes waves. Therefore, each Stokes wave will compete with the others, which leads to the intensity ratio of different Stokes waves varying with the change of pump power. On the whole, as the pump power increases, the higher-order Stokes light gradually dominates. First, the fundamental frequency light dominates. Then, the 1st-order Stokes wave begins to dominate, and finally the 6th-order Stokes dominates. The maximum power of 1st-order to 7th-order Stokes waves are ~615 mW, ~418 mW, ~312 mW, ~412 mW, ~642 mW, ~823 mW, and ~613 mW calculated according to the output spectral intensity ratio of different wavelengths.

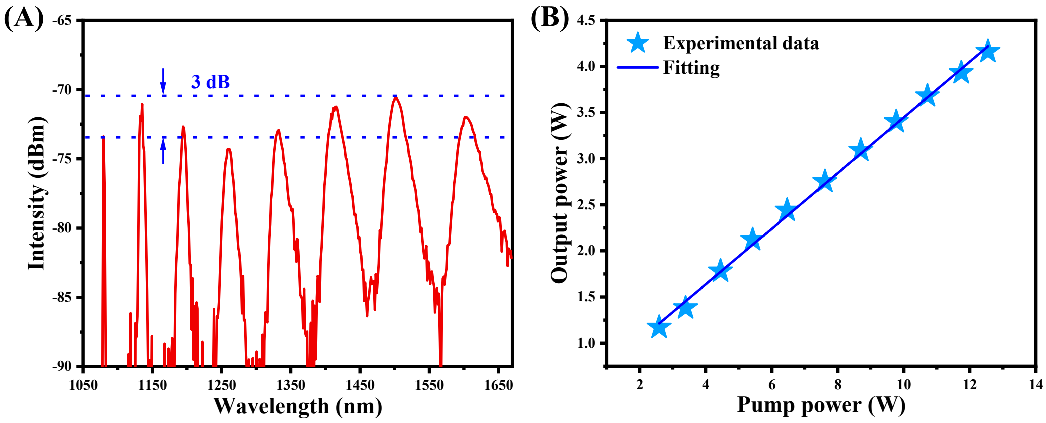

Figure 2. (**A**) Optical spectrum of the multi-wavelength RRFL; (**B**) Total output power of the multi-wavelength RRFL.

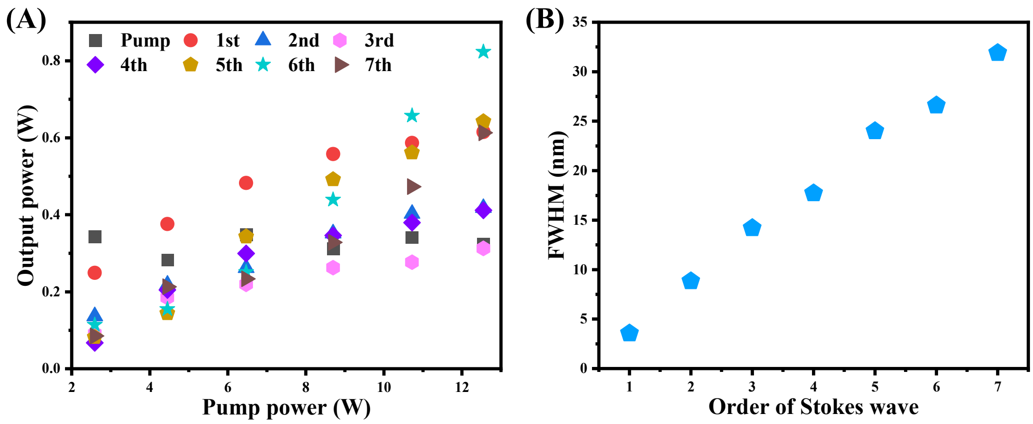

Figure 3. (**A**) Output power of different Stokes waves; (**B**) FWHM of different Stokes waves.

The optical spectra of each Stokes wave are tested and analyzed. The FWHM of the optical spectrum increases with increases in Stokes waves' order. As shown in Figure 3B, the FWHM of the 7th-order Stokes wave can reach 31.9 nm, and that of the 1st-order Stokes wave is only 3.57 nm. In particular, the multi-wavelength phenomenon is not only obtained in a wide range from 1.1–1.6 μm but also observed in the optical spectra of 1st-order and 2nd-order Stokes waves. And Figure 4A,B, respectively, exhibit their fine optical spectra under a resolution of 0.05 nm. For the 1st-order Stokes wave, four wavelength peaks are recorded in the 3-dB bandwidth of the optical spectrum, which is 3.57 nm, and the average wavelength spacing is 1 nm. For the 2nd-order Stokes wave, there are 20 peaks in its 3-dB bandwidth of the optical spectrum, which is 8.84 nm, and the average wavelength spacing decreases to 0.45 nm. However, this phenomenon is not observed in other Stokes waves, which is mainly due to the spectral broadening of high-order Stokes waves making these subtle modulations difficult to distinguish as the peaks with small spacing connected together in the process of Raman frequency shift. As we know, the formation mechanism of 1st-order to 7th-order Stokes waves is stimulated Raman scattering. However, the peaks located on the 1st-order and 2nd-order Stokes waves are mainly caused by the filtering effect of fiber loop mirror combined with the random distributed feedback from the 1-km-long Raman optical fiber and FWM [28,29], which is different from the multi-wavelength operation of the seven Stokes waves.

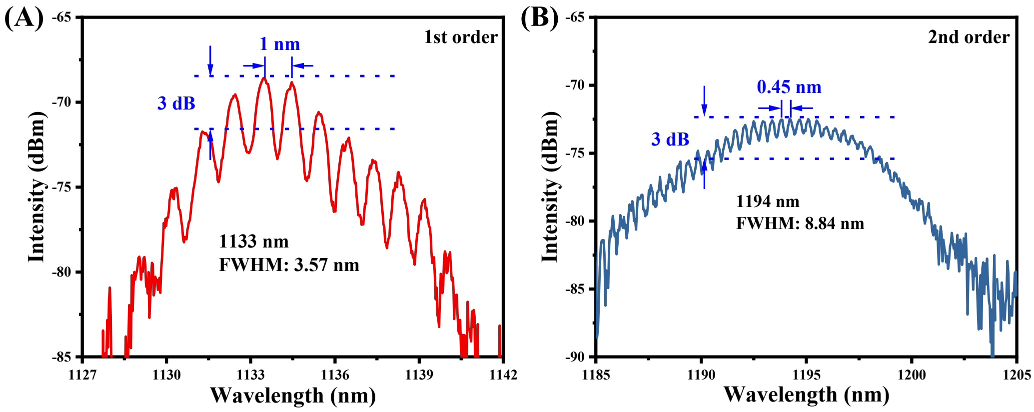

Figure 4. (**A**) Optical spectrum of the 1st-order Stokes wave; (**B**) Optical spectrum of the 2nd-order Stokes wave.

4. Conclusions

In conclusion, a seven-wavelength random Raman fiber laser in the range of 1.1–1.6 μm is realized in this work. The 1st-order to 7th-order Stokes waves are located at 1133 nm, 1194 nm, 1260 nm, 1332 nm, 1414 nm, 1504 nm, and 1606 nm, respectively, corresponding to the maximum output power of ~615 mW, ~418 mW, ~312 mW, ~412 mW, ~642 mW, ~823 mW, and ~613 mW. In the 3 dB bandwidth of optical spectra of 1st-order and 2nd-order Stokes waves, four peaks with an average spacing of 1 nm and 20 peaks with an average spacing of 0.45 nm are recorded, respectively. This work is expected to be applied in the fields of multi-species gas monitoring, WDM, and fiber sensors through subsequent improvement and testing.

Author Contributions: Conceptualization, C.H. and P.S.; methodology, C.H. and P.S.; validation, C.H.; formal analysis, C.H.; investigation, C.H.; resources, P.S.; writing—original draft preparation, C.H.; writing—review and editing, P.S.; supervision, P.S.; project administration, P.S.; funding acquisition, P.S. All authors have read and agreed to the published version of the manuscript.

Funding: This research was funded by National Natural Science Foundation of China (61975099).

Institutional Review Board Statement: Not applicable.

Informed Consent Statement: Not applicable.

Data Availability Statement: The data presented in this study are available upon reasonable request.

Conflicts of Interest: The authors declare no conflict of interest.

References

1. Adamu, A.I.; Wang, Y.; Habib, M.S.; Dasa, M.K.; Antonio-Lopez, J.E.; Amezcua-Correa, R.; Bang, O.; Markos, C. Multi-wavelength high-energy gas-filled fiber Raman laser spanning from 1.53 μm to 2.4 μm. *Opt. Lett.* **2021**, *46*, 452–455. [CrossRef]
2. Sugavanam, S.; Yan, Z.; Kamynin, V.; Kurkov, A.S.; Zhang, L.; Churkin, D.V. Multiwavelength generation in a random distributed feedback fiber laser using an all fiber Lyot filter. *Opt. Express* **2014**, *22*, 2839–2844. [CrossRef] [PubMed]
3. Wang, Z.N.; Wu, H.; Fan, M.Q.; Li, Y.; Gong, Y.; Rao, Y.J. Broadband flat-amplitude multiwavelength Brillouin-Raman fiber laser with spectral reshaping by Rayleigh scattering. *Opt. Express* **2013**, *21*, 29358–29363. [CrossRef] [PubMed]
4. Du, X.Y.; Zhang, H.W.; Wang, X.; Wang, X.L.; Zhou, P.; Liu, Z.J. Multiwavelength Raman fiber laser based on polarization maintaining fiber loop mirror and random distributed feedback. *Laser Phys. Lett.* **2015**, *12*, 45106. [CrossRef]
5. Fernandez-Vallejo, M.; Díaz, S.; Perez-Herrera, R.A.; Passaro, D.; Selleri, S.; Quintela, M.A.; López Higuera, J.M.; Lopez-Amo, M. Resilient long-distance sensor system using a multiwavelength Raman laser. *Meas. Sci. Technol.* **2010**, *21*, 94017. [CrossRef]
6. Han, Y.G.; Tran, T.V.; Kim, S.H.; Lee, S.B. Multiwavelength Raman-fiber-laser-based long-distance remote sensor for simultaneous measurement of strain and temperature. *Opt. Lett.* **2005**, *30*, 1282–1284. [CrossRef]
7. Luo, Z.Q.; Cai, Z.P.; Huang, J.F.; Ye, C.C.; Huang, C.H.; Xu, H.Y.; Zhong, W.D. Stable and spacing-adjustable multiwavelength Raman fiber laser based on mixed-cascaded phosphosilicate fiber Raman linear cavity. *Opt. Lett.* **2008**, *33*, 1602–1604. [CrossRef] [PubMed]
8. Pan, S.L.; Lou, C.Y.; Gao, Y.Z. Multiwavelength erbium-doped fiber laser based on inhomogeneous loss mechanism by use of a highly nonlinear fiber and a Fabry-Perot filter. *Opt. Express* **2006**, *14*, 1113–1118. [CrossRef] [PubMed]

9. Wang, F.; Zhang, X.L.; Yu, Y.; Huang, X. 82-channel multi-wavelength comb generation in a SOA fiber ring laser. *Opt. Laser Technol.* **2010**, *42*, 285–288. [CrossRef]
10. Yuan, Y.J.; Yao, Y.; Yi, M.; Guo, B.; Tian, J.J. Multiwavelength fiber laser employing a nonlinear Brillouin optical loop mirror: Experimental and numerical studies. *Opt. Express* **2014**, *22*, 15352–15363. [CrossRef]
11. Shirazi, M.R.; Mohamed Taib, J.; Dimyati, K.; Harun, S.W.; Ahmad, H. Multi-wavelength Brillouin–Raman fiber laser generation assisted by multiple four-wave mixing processes in a ring cavity. *Laser Phys.* **2013**, *23*, 75108. [CrossRef]
12. Ahmad, H.; Parvizi, R.; Dimyati, K.; Tamjis, M.R.; Harun, S.W. FWM-based multi-wavelength erbium-doped fiber laser using Bi-EDF. *Laser Phys.* **2010**, *20*, 1414–1417. [CrossRef]
13. Zhang, L.N.; Yan, F.P.; Feng, T.; Guo, Y.; Qin, Q.; Zhou, H.; Suo, Y.P. Switchable Multi-Wavelength Thulium-Doped Fiber Laser Employing a Polarization-Maintaining Sampled Fiber Bragg Grating. *IEEE Access* **2019**, *7*, 155437–155445. [CrossRef]
14. Yeh, C.H.; Chow, C.W.; Wu, Y.F.; Shih, F.Y.; Wang, C.H.; Chi, S. Multiwavelength erbium-doped fiber ring laser employing Fabry–Perot etalon inside cavity operating in room temperature. *Opt. Fiber Technol.* **2009**, *15*, 344–347. [CrossRef]
15. Wang, M.; Huang, Y.J.; Yu, L.; Song, Z.P.; Liang, D.Z.; Ruan, S.C. Multiwavelength Thulium-Doped Fiber Laser Using a Micro Fiber-Optic Fabry–Perot Interferometer. *IEEE Photon. J.* **2018**, *10*, 1–8. [CrossRef]
16. Sierra-Hernandez, J.M.; Rojas-Laguna, R.; Vargas-Rodriguez, E.; Estudillo-Ayala, J.M.; Mata-Chavez, R.I.; Jauregui-Vazquez, D.; Hernandez-Garcia, J.C.; Andrade-Lucio, J.A.; Gutierrez-Gutierrez, J.C. A tunable multi-wavelength laser based on a Mach–Zehnder interferometer with photonic crystal fiber. *Laser Phys.* **2013**, *23*, 55105. [CrossRef]
17. Liu, S.; Yan, F.P.; Wu, B.L.; Tan, S.Y.; Peng, W.J.; Feng, T.; Liang, X.; Li, Q. A multiwavelength thulium-doped silica fiber laser incorporating a highly nonlinear fiber. *J. Opt.* **2014**, *16*, 55201. [CrossRef]
18. Liu, D.; Ngo, N.Q.; Liu, H.; Liu, D. Stable multiwavelength fiber ring laser with equalized power spectrum based on a semiconductor optical amplifier. *Opt. Commun.* **2009**, *282*, 1598–1601. [CrossRef]
19. Pleros, N.; Bintjas, C.; Kalyvas, M.; Theophilopoulos, G.; Yiannopoulos, K.; Sygletos, S.; Avramopoulos, H. Multiwavelength and power equalized SOA laser sources. *IEEE Photon. Technol. Lett.* **2002**, *14*, 693–695. [CrossRef]
20. Liang, D.M.; Xu, X.F.; Li, Y.; Pei, J.H.; Jiang, Y.; Kang, Z.H.; Gao, J.Y. Multiwavelength fiber laser based on a high-birefringence fiber loop mirror. *Laser Phys. Lett.* **2007**, *4*, 57–60. [CrossRef]
21. Frazão, O.; Correia, C.; Santos, J.L.; Baptista, J.M. Raman fibre Bragg-grating laser sensor with cooperative Rayleigh scattering for strain–temperature measurement. *Meas. Sci. Technol.* **2009**, *20*, 45203. [CrossRef]
22. Kim, C.S.; Sova, R.M.; Kang, J.U. Tunable multi-wavelength all-fiber Raman source using fiber Sagnac loop filter. *Opt. Commun.* **2003**, *218*, 291–295. [CrossRef]
23. Turitsyn, S.K.; Babin, S.A.; El-Taher, A.E.; Harper, P.; Churkin, D.V.; Kablukov, S.I.; Ania-Castañón, J.D.; Karalekas, V.; Podivilov, E.V. Random distributed feedback fibre laser. *Nat. Photonics* **2010**, *4*, 231–235. [CrossRef]
24. Balaswamy, V.; Arun, S.; Aparanji, S.; Choudhury, V.; Supradeepa, V.R. High-power, fixed, and tunable wavelength, grating-free cascaded Raman fiber lasers. *Opt. Lett.* **2018**, *43*, 1574–1577. [CrossRef] [PubMed]
25. Jiang, H.; Zhang, L.; Feng, Y. Silica-based fiber Raman laser at >2.4 µm. *Opt. Lett.* **2015**, *40*, 3249–3252. [CrossRef]
26. Liu, J.; Tan, F.; Shi, H.; Wang, P. High-power operation of silica-based Raman fiber amplifier at 2147 nm. *Opt. Express* **2014**, *22*, 28383–28389. [CrossRef]
27. Jin, X.; Lou, Z.; Zhang, H.; Xu, J.; Zhou, P.; Liu, Z. Random distributed feedback fiber laser at 2.1 µm. *Opt. Lett.* **2016**, *41*, 4923–4926. [CrossRef]
28. El-Taher, A.E.; Harper, P.; Babin, S.A.; Churkin, D.V.; Podivilov, E.V.; Ania-Castanon, J.D.; Turitsyn, S.K. Effect of Rayleigh-scattering distributed feedback on multiwavelength Raman fiber laser generation. *Opt. Lett.* **2011**, *36*, 130–132. [CrossRef]
29. Pinto, A.M.R.; Frazão, O.; Santos, J.L.; Lopez-Amo, M. Multiwavelength fiber laser based on a photonic crystal fiber loop mirror with cooperative Rayleigh scattering. *Appl. Phys. B* **2010**, *99*, 391–395. [CrossRef]